Capacity Enhancement in Irregular RIS-Assisted Wireless Networks Using Standard and Improved Particle Swarm Optimization

Imran A. Khoso, Zhou He, Yejun He, *Senior Member, IEEE*, Mohsen Guizani, *Fellow, IEEE*

***Abstract*—Reconfigurable Intelligent Surface (RIS) enhances the performance of wireless networks by smartly reconfiguring the wireless propagation environment. This enhancement is highly dependent on the number of RIS elements, but practical challenges like high channel acquisition overhead and power consumption limit the scalability of traditional RIS systems. Recently proposed irregular RIS has been shown to tackle these challenges effectively. However, its potential advantages are not fully realized since the topology and precoding designs are alternatively optimized, which does not consider the impact of topology changes on precoding. In this paper, we leverage the benefits of irregular RIS and propose new approaches to exploit its potential fully. The key idea is to enhance the system capacity by enabling simultaneous optimization of the irregular RIS topology and precoding design. Specifically, we propose the standard particle swarm optimization (PSO) algorithm to jointly optimize the RIS topology, beamforming, and reflection coefficients. Unlike the conventional approach, PSO simultaneously evaluates potential solutions via particle updates that enhance the system capacity significantly. Next, we introduce an improved variant of PSO, designed to improve the exploration-exploitation tradeoff and speed up the convergence. Specifically, the improved PSO approach enables the dynamic adjustments of PSO parameters throughout the process, reducing the risk of premature convergence and significantly improving the overall performance compared to the standard PSO. The effectiveness of the proposed improved PSO is validated through a complex multi-modal Michalewicz function benchmark test, which illustrates that the obtained results are virtually the same as the expected results for different dimensional spaces. Besides, we also provide convergence and complexity analysis of the improved PSO. Numerical results and analysis demonstrate that the proposed algorithms significantly enhance the system capacity with low complexity by simultaneously optimizing the topology and precoding design.**

***Index Terms*—Particle swarm optimization (PSO), Reconfigurable Intelligent Surface (RIS), irregular RIS, precoding, optimization.**

Manuscript received Mar. 13, 2025, revised July 20, 2025, accepted Sept. 29, 2025. This work was supported in part by the National Key Research and Development Program of China under Grant 2023YFE0107900, in part by the National Natural Science Foundation of China under Grant 62071306, in part by the National Key Research and Development Program of China under Grant 2023YFE0107900, and n part by the Key Program of Shenzhen Natural Science Foundation under grant JCYJ20241202124219023. (Corresponding author: Yejun He.)

Imran A. Khoso and Yejun He are with Guangdong Engineering Research Center of Base Station Antennas and Propagation, Sino-British Antennas and Propagation Joint Laboratory of Ministry of Science and Technology of China, the State Key Laboratory of Radio Frequency Heterogeneous Integration, Shenzhen Key Laboratory of Antennas and Propagation, College of Electronics and Information Engineering, Shenzhen University, Shenzhen 518060, China (e-mail: imrankhoso2@gmail.com, heyejun@126.com).

Zhou He is with the Department of Mechanical Engineering, University of Maryland, College Park, MD 20742 USA (e-mail: zhe12@umd.edu).

Mohsen Guizani is with the Machine Learning Department, Mohamed Bin Zayed University of Artificial Intelligence (MBZUAI), Abu Dhabi 99163, UAE (e-mail: mguizani@ieee.org).

I. Introduction

The fifth-generation (5G) mobile communication systems have been deployed worldwide recently, addressing the key challenges in transmission capacity, latency, and reliability. However, high-quality service requirements of emerging applications such as the internet of everything (IoE), intelligent transportation systems, autonomous systems, and immersive virtual reality cannot be readily supported by existing 5G communication systems [1], [2]. Thus, the wireless industry is casting its eyes on future sixth-generation (6G) wireless systems that is expected to meet the demands of next-generation technologies such as ultra high energy efficiency and data rate, extremely low latency and high reliability, and global coverage and connectivity [3], [4]

Among candidate technologies at a nascent research stage for future wireless systems, Reconfigurable Intelligent Surface (RIS)-aided systems have attracted a lot of research attention recently [5]–[7] and have been recognized as a cost-effective complement [8]. It is a two-dimensional metasurface that creates or shapes the propagation environment by manipulating the electromagnetic waves, thus enhancing wireless communication. RIS consists of several sub-wavelength-sized elements, each capable of scattering and shifting the phase of incoming waves [9]. The pattern of phase-shift among the elements determines the desired direction of reflection elements [10], [11]. Recent advancements in metamaterials [12] have enabled the real-time reconfiguration of phase shifts. Consequently, the phase shifts of all reflective elements can be adjusted collaboratively, allowing the reflected signals from the RIS to be either destructively or constructively added at the receiver. This capability allows for the beneficial steering of the signal component that arrives from the base station (BS) to either suppress unwanted signals such as interference or enhance the power of the desired signal. Thus, unlike traditional wireless networks, where information is sent from a transmitter to a receiver in an uncontrolled propagation environment, RIS allows the creation of real-time reconfigurable propagation environments, transforming the propagation environment into an intelligent and controllable entity [6], [12]. RIS can be densely deployed with low energy consumption scalable costs since it operates over a short range and eliminates the need for transmit RF chains. It can be coated easily in buildings, walls, ceilings, and facades because of its low weight and small size. In addition, RISs are passive elements, eliminating the

use of sophisticated interference management among them. Considering its appealing advantages, a lot of research has been focusing on RIS-assisted communication systems [13].

In this regard, RIS was exploited to improve wireless transmission rates and coverage by controlling the propagation environment in [14]. Considering the signal-to-interference-plus-noise (SINR) constraints, a joint optimization of transmit and reflect beamforming is proposed to minimize the system's transmission power [15]. Later, many works considered the optimization of RIS to enhance system performance. As such, the energy and spectrum efficiency of a RIS-assisted multiple-input single-output (MISO) system was investigated by adjusting the number of reflecting elements at the RIS and the transmit power [16]. The RIS was investigated to minimize the SINR outage probability [17] or to maximize the signal-to-leakage-ratio [18] under power and unit modulus constraints. In [19], [20], multiple-input multiple-output (MIMO) systems were optimized using both passive and active beamforming, which aims to maximize the achievable rate. The energy efficiency in the RIS-assisted MIMO systems has been studied by jointly designing the transmit beamforming and reflecting coefficient in [21]–[23] and spectrum efficiency and energy efficiency tradeoff was studied in [24]. Moreover, a beamforming design with imperfect CSI for an RIS-assisted system was investigated in [25] to ensure the service quality by jointly optimizing the RIS placement, passive beamforming, and transmit beamforming of the BS. Moreover, particle swarm optimization (PSO) for optimizing various aspects of RIS-assisted networks has been studied recently. For instance, PSO was applied to jointly optimize unmanned aerial vehicle (UAV) trajectory and RIS phase shifts for maximizing sum rates in aerial networks [26], while [27] utilized PSO algorithms to enhance energy efficiency and secrecy rates in UAV-RIS systems. Additionally, PSO-based approach has been employed for optimizing simultaneous transmission and reflection (STAR)-RIS configurations in non-orthogonal multiple access (NOMA) systems, focusing on beamforming design and power allocation [28]. In the context of energy-efficient communications, [29] proposed beamforming optimization for MISO systems where PSO is used to optimize RIS element switching matrices. Furthermore, [30] presented a low-complexity joint active and passive beamforming approach for RIS-aided MIMO systems, where PSO algorithm was exploited to solve the non-convex sum-rate optimization problem. Though, in the literature, RIS-assisted wireless systems have been extensively studied, most of these studies have focused on the regular RIS. The elements in regular RIS are arranged regularly on a grid where inter-element spacing is constant. The performance of RIS-assisted systems is heavily dependent on the number of reflecting elements, which means increasing the number of RIS elements will only enhance array gain. Nevertheless, the number of RIS elements in practical systems is typically limited due to high power consumption and overhead of channel acquisition.

Recently, a new concept considering irregular RIS structure has been introduced to enhance the capacity of RIS-aidedd systems with a limited number of RIS elements [31]. To improve weighted sum rate (WSR) of a system, a joint topology optimization and precoding design problem was formulated, and an alternative optimization method was used to solve it. Specifically, the iterative Tabu search (ATS) approach is utilized for topology design and then, for a given topology, a neighbour extraction-based cross-entropy (NECE) is applied for precoding design. Although this work successfully improved the capacity of wireless system but it has several limitations. First, it relies on alternative optimization approach that does not simultaneously consider the impact of topology changes on the precoding but rather they are decoupled and optimized separately. This prevents the full exploration of the interdependencies between variables. This kind of alternating optimization techniques typically converge to the local optimum [32], [33] and leads to suboptimal results due to interdependencies between RIS topology and precoding. Additionally, both ATS and NECE approaches are prone to getting trapped in local minima. ATS, being a local search scheme, may lead to suboptimal solutions in complex search spaces. NECE may also converge to similar suboptimal solutions since it can be limited by its neighbourhood-based search. Furthermore, both methods suffer from high computational complexity as the number of RIS elements or users increases. ATS requires a large number of iterations for topology design, while NECE requires multiple iterations to obtain desired results for precoding design, which makes the overall process computationally expensive for RIS-assisted large antenna systems. In addition, when applying conventional alternative optimization method in systems where a higher number of RIS elements and antennas are considered, the benefits of exploiting an irregular RIS topology become less pronounced, and both the regular RIS and irregular RIS configurations tend to yield similar performance outcomes. This is because these methods struggle to fully exploit the additional degrees of freedom the irregular RIS offers. Hence, the potential advantages of an irregular RIS topology are not fully realized. In parallel to irregular RIS research, the concept of shape-adaptive reconfigurable holographic surfaces (RHS) has recently been proposed [34]. Unlike conventional RIS, which operate using passive phase-shifting elements, RHS enables the dynamic selection of active surface regions from a set of predefined shapes to optimize signal propagation. This allows RHS to achieve spatial adaptability and enhanced performance with lower element control overhead. While our work focuses on irregular RIS, the core motivation of enabling geometric flexibility aligns closely with RHS. However, our approach remains more compatible with existing RIS implementations and avoids the hardware complexity associated with holographic feeds.

Motivated by the abovementioned issues, in this paper, we focus on effective solutions for irregular RIS-assisted wireless networks. We consider the joint design of the irregular RIS topology and precoding (beamforming at the BS and the phase shifts at the RIS). Since the optimization problem is a mixed integer non-convex, we propose a PSO method to solve it where the RIS topology and precoding design are simultaneously optimized in each iteration until desired results are achieved. PSO does not rely on convexity or gradient information which makes it suitable for irregular RIS-

assisted high-dimensional systems where the joint topology and precoding design lead to a non-linear objective function. Unlike ATNE (for simplicity, we will henceforth refer to the conventional ATS and NECE-based alternative optimization method [31] as ATNE), which alternatively updates each design component, PSO simultaneously evaluates potential solutions via particle updates within a single optimization framework. As a consequence of this simultaneous approach, PSO can explore a wider search space with fewer iterations and significantly achieve better performance than the alternative optimization method. Thus, PSO offers a powerful method to address the complex inter-dependencies of the multiuser irregular RIS-assisted communication system. In addition, the hyperparameters of PSO such as particle count, social/cognitive coefficients, and inertia weight can be easily adjusted to adapt to different user requirements or network conditions. This adaptability is beneficial in dynamic irregular RIS-assisted wireless environments where RIS configurations need to be updated frequently. The parameters in the standard PSO approach such as the inertia weight, and cognitive and social coefficients are fixed throughout the optimization process. Though this simplicity can be effective, it often leads to premature convergence or ineffective exploration, especially in non-linear high-dimensional optimization problems. To overcome this limitation, we introduce an improved PSO algorithm that provides substantial improvements compared to the standard PSO by dynamically adjusting parameters throughout optimization process, leading to more accurate solutions and better convergence rates. By exploiting the dynamic nature of the parameters, we can efficiently manage the interdependencies between the RIS topology, phase shift design and beamforming, enhancing overall performance in solving the complicated multivariant optimization problem. While PSO is traditionally considered a metaheuristic approach, its applicability in wireless systems largely depends on the optimization timescale. In scenarios where RIS topology and beamforming do not require frequent updates, such as slowly varying environments or during system initialization, PSO offers a practical and effective solution. Moreover, the parallel structure of the algorithm enables acceleration through modern hardware platforms. Therefore, the proposed PSO approach achieves a favorable balance between performance and computational complexity. Our main contributions can be summarized as follows:

- We propose a more integrated approach to simultaneously optimize RIS topology and precoding design, compensating for performance loss of the conventional alternating optimization approach. The joint optimization problem, formulated to enhance MIMO channel capacity, is multivariate and non-convex. We propose to exploit PSO algorithm to solve this problem.
- We introduce a new variant of the PSO that allows the inertia weight, social coefficient, and cognitive coefficient to change adaptively throughout the process. We provide generalized improved PSO algorithm that is well-suited for optimization tasks across various domains. To show its efficacy, it is applied to solve the joint optimization problem of irregular RIS topology and precoding design. The improved PSO algorithm is validated using the multi-modal Michalewicz function, and the impact of the non-stationary nature of its parameters is analyzed.
- We analyze the theoretical convergence and associated complexity of the improved PSO algorithm. The analysis demonstrates that the proposed PSO algorithm exhibits lower complexity compared to the conventional method.

Numerical results are provided to validate the performance superiority of the proposed algorithms, which show that the proposed standard PSO and the improved PSO algorithms significantly enhance the overall capacity of the irregular RIS-assisted wireless communication system.

The rest of the paper is organized as follows. Section II describes the RIS-aided multi-user MIMO system model and discusses the formulation of the problem. In Section III, we propose PSO optimization method to enhance the capacity of wireless systems. In addition, an improved PSO is introduced and applied to the problem in hand in this section. The multi-modal Michalewicz function test, convergence analysis and complexity are discussed in Section-IV to validate the improved PSO algorithm. To verify the superiority of the proposed methods, we provide simulation results in Section-V. Finally, section VI concludes the paper.

II. System Model and Problem Formulation

We consider an irregular RIS-aided multiuser MIMO downlink communication system as shown in Figure 1, where a BS employing M transmitting antennas and serving K single-antenna users simultaneously. The BS and users communicate through RIS that deploys N reflecting elements distributed irregularly over N_s grid points of an enlarged surface, where N_s must be greater than N. For simplicity, spacing between the grid points assumed to be fixed and it is half the carrier frequency wavelength without loss of generality. The system benefits from both reflected and direct paths, providing additional diversity and improving the communication quality. Thus, the signals received by each user is a superposition of the signals transmitted through both the RIS-assisted and the direct links. The RIS-assisted MIMO system enables the BS to operate with significantly less number of antennas while still maintaining high-quality user service in contrast to massive MIMO systems with hundreds of active antennas [35]. This is achieved by exploiting the RIS's large aperture to generate finely-grained reflected beams through smart passive reflections.

For accounting the small-scale fading, we adopt the Rician fading channel model. The channel between the BS and RIS can be written by

$$G = \sqrt{\frac{\omega_{BR}}{1+\omega_{BR}}} G_{\text{LoS}} + \sqrt{\frac{1}{1+\omega_{BR}}} G_{\text{NLoS}}, \tag{1}$$

where ω_{BR} stands for the Rician factor, G_{LoS} and G_{NLoS} denote line-of-sight (LoS) and Non-LoS (NLoS) (Rayleigh fading) component, respectively. Particularly, this model can become the LoS channel when $\omega_{BR} \to \infty$, or Rayleigh fading when $\omega_{BR} = 0$. Similarly, by following the same procedure,

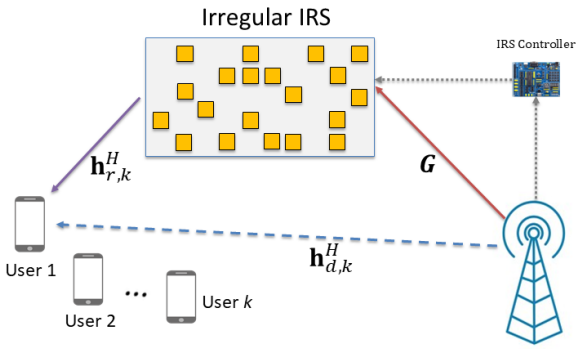

Fig. 1. Irregular RIS-assisted wireless communication system

the RIS-User and BS-User channels can be generated. The large-scale fading, i.e., the path loss that is affected by distance, is also considered that, for the BS-RIS-UE channel, can be expressed as follows [15], [36]

$$f_r(d_{BR}, d_{RU}) = C_{\mathrm{r}} \cdot d_{BR}^{-\beta_{BR}} \cdot d_{RU}^{-\beta_{RU}}, \tag{2}$$

where the distances between the RIS and users are denoted by d_{RU} and the RIS and BS by d_{BR}, respectively. C_r stands for the impact of antenna gain and channel fading. BS-user channel path loss can similarly be written as

$$f_d(d_{BU}) = C_{\mathrm{d}} \cdot d_{BU}^{-\beta_{BU}}. \tag{3}$$

where C_d is channel fading and antenna gain coefficient for direct links.

Let $\mathbf{s}_k$ is the information-bearing transmitted symbol, $\mathbf{h}_d^H \in \mathbb{C}^{1\times M}$ denotes the direct channel between the BS and user k and $\mathbf{w}_k \in \mathbb{C}^{M\times 1}$ is the beamforming vector for user k. Then the received signal $\mathbf{y}_k$ by user k from the direct path can be expressed as

$$y_{d,k} = \mathbf{h}_d^H \mathbf{w}_k s_k + \sum_{j\neq k} \mathbf{h}_d^H \mathbf{w}_j s_j + n_k, \tag{4}$$

where $n_k \sim \mathcal{CN}(0, \sigma^2)$ is the additive white Gaussian noise (AWGN).

The RIS receives the signal from the BS and reflects towards users, which introduces an additional path. Let $\mathbf{T} = \mathrm{diag}(t_1, t_2, \ldots, t_N)$ denotes the topology matrix that represents the topology of RIS, where $t_n \in \{0, 1\}$ indicate whether the n-th grid position is active (where $n = 1, 2, ..., Ns$). Specifically, $t_n = 0$ indicates that no RIS element is selected for n-th grid point while $t_n = 1$ denotes that the RIS element is selected for the n-th grid point. The effective channel for user k can thus be reformulated as

$$\mathbf{h}_k = \mathbf{h}_d + \mathbf{h}_r \mathbf{T}\boldsymbol{\Theta}\mathbf{G}, \tag{5}$$

and consequently, the signal received through RIS-assisted path can be written as

$$y_{r,k} = \mathbf{h}_k \mathbf{w}_k s_k + \sum_{j\neq k} \mathbf{h}_j \mathbf{w}_j s_j + n_k, \tag{6}$$

where $\mathbf{h}_r^H \in \mathbb{C}^{1\times N}$ and $\mathbf{G} \in \mathbb{C}^{N\times M}$ represent the channel between the RIS and user k and the channel between the BS and the RIS, respectively, and the diagonal reflection-coefficient matrix $\boldsymbol{\Theta}$ at the RIS can be denoted as

$$\boldsymbol{\Theta} = \mathrm{diag}\left(\left[\beta_1 e^{j\theta_1}, \beta_2 e^{j\theta_2}, \ldots \beta_{Ns} e^{j\theta_{Ns}}\right]\right), \tag{7}$$

where β and $\theta_n \in \{0, 1\}$ are, respectively, the amplitude of reflection and the phase shift of the n-th RIS element. Both the amplitude of reflection coefficients and the phase shift of RIS elements can independently be controlled at a time [33], [37]. The reflection amplitude β_n satisfies $\beta_n = 1$ for $\forall n = 1, 2, ...N_s$ [31], and binary phase shifts $\{0, 1\}$ are considered for the RIS elements, where 1 and 0 represent an active element and an inactive element. While continuous phase shifts offer theoretically better beamforming flexibility, binary phase shifts offers several practical benefits such as simplified hardware implementation as elements just need ON/OFF states, minimal control overhead (1-bit per element), eliminate phase calibration requirements and compatibility with low-cost digital controllers [38]. From a computational viewpoint, the binary phase shifts lead to a simpler optimization problem with lower computational complexity and faster convergence compared to continuous phase shifts.

The total received signal for user k, which is a combination of the direct link without RIS and the indirect RIS-assisted paths, can be expressed as

$$y_k = \left(\mathbf{h}_d^H + \mathbf{h}_r^H \boldsymbol{\Theta}\mathbf{G}\right) \mathbf{w}_k s_k + \sum_{j\neq k} \left(\mathbf{h}_d^H + \mathbf{h}_r^H \boldsymbol{\Theta}\mathbf{G}\right) \mathbf{w}_j s_j + n_k, \tag{8}$$

and the signal received $\mathbf{y}_k \in \mathbb{C}^{K\times 1}$ for all K users is

$$y = \left(\mathbf{H}_r^H \mathbf{T}\boldsymbol{\Theta}\mathbf{G} + \mathbf{H}_d^H\right) \mathbf{s} + \mathbf{n}, \tag{9}$$

where $\mathbf{s}$ is the superimposed symbol which is a combination of all transmitted symbols, $\mathbf{y} = [y_1, y_2, \ldots, y_K]^T$ represents the received signal vector for all users, $\mathbf{H}_r = [\mathbf{h}_{r,1}, \mathbf{h}_{r,2}, \ldots, \mathbf{h}_{r,K}]^H \in \mathbb{C}^{K\times N_S}$ and $\mathbf{H}_d = [\mathbf{h}_{d,1}, \mathbf{h}_{d,2}, \ldots, \mathbf{h}_{d,K}]^H \in \mathbb{C}^{K\times M}$ are RIS-assisted BS to users and the direct BS to users channel matrices, respectively, and $\mathbf{n} = [n_1, n_2, \ldots, n_K]^T$ is the AWGN vector.

For the given irregular RIS-assisted communication system, we can express the signal-to-interference-plus-noise ratio (SINR) of user k as

$$\mathrm{WSR} = \sum_{k=1}^{K} \alpha_k \log_2\left(1 + \mathrm{SINR}_k\right), \tag{10}$$

where α_k represents the weight assigned to user k and SINR_k for user k defined as:

$$\mathrm{SINR}_k = \frac{|\left(\mathbf{h}_d^H + \mathbf{h}_r^H \mathbf{T}\boldsymbol{\Theta}\mathbf{G}\right) \mathbf{w}_k|^2}{\sum_{j\neq k} |\left(\mathbf{h}_d^H + \mathbf{h}_r^H \mathbf{T}\boldsymbol{\Theta}\mathbf{G}\right) \mathbf{w}_j|^2 + \sigma^2}. \tag{11}$$

The overall capacity of the wireless system can be enhanced by optimizing the SINR across all users. Our objective is maximizing the WSR of K single-antenna users served by a BS employing M number of antennas by exploiting the irregular RIS strategy.

Next, the optimization problem is formulated for maximizing the WSR in an irregular RIS-assisted multi-user MIMO

system. The performance of an irregular RIS-assisted wireless system can be enhanced greatly by carefully designing its topology and precoding design. Irregular RIS topology provides greater flexibility but it is challenging to jointly design the optimal RIS topology (active/inactive state of each grid position) and precoding matrix to maximize the WSR for all users.

Since fully digital precoder $\mathbf{W} = [w_1, w_2, \ldots, w_K]$ is considered at the BS, BS transmit power can be represented as

$$P = \sum_{k=1}^{K} \|\mathbf{w}_k\|_2^2. \tag{12}$$

BS transmit power is limited by the maximum transmit power $P_{\max}$ such as $P \leq P_{\max}$. We consider that the phase shift of each RIS element is binary, where 1 shows an active element and 0 represents an inactive element. We further assume that the phase shifts directly linked to its topology state such as

$$\theta_n = t_n, \quad \forall n = 1, 2, ...N_s. \tag{13}$$

Our primary objective is to maximize the WSR by jointly optimizing the RIS topology, the beamforming at the BS, and the RIS phase shifts. Thus, the WSR maximization problem for considered RIS-assisted system with some practical constraints can be stated as

$$\max_{\mathbf{T},\mathbf{W},\mathbf{\Theta}} \quad \sum_{k=1}^{K} \alpha_k \log_2 (1 + \text{SINR}_k) \tag{14a}$$

$$\text{subject to} \quad |\mathbf{W}|_F^2 \leq P_{\max}, \tag{14b}$$

$$\theta_n \in \{0, 1\}, \quad \forall n = 1, 2, ...N_s \tag{14c}$$

$$t_n \in \{0, 1\}, \quad \forall n = 1, 2, ...N_s \tag{14d}$$

$$\theta_n = t_n, \quad \forall n, \tag{14e}$$

$$\sum_{n=1}^{N_S} t_n = N. \tag{14f}$$

where $|\mathbf{W}|_F^2 \leq P_{\max}$ and $\theta_n = \{0, 1\}$ are the the Frobenius norm power and phase shift constraints, respectively. Here $\theta_n = t_n$ indicates that the phase shift of each RIS element is binary and directly linked to its topology state which enforces hardware consistency, when an element is active ($t_n = 1$), it implements a phase shift of zero degree ($e^{j0} = 1$), and when inactive ($t_n = 0$), it implements no reflection. This matches practical RIS implementations that synchronize element activation and phase states through single-bit control. This simplification allows us to jointly represent the topology and phase shift design through a single binary matrix $\mathbf{T}$, where the diagonal elements of $\mathbf{\Theta}$ directly correspond to the topology states. $t_n \in \{0, 1\}$ and $\sum_{n=1}^{N_S} z_n = N$ correspond to the irregular RIS topology constraints. The irregular topology constraints regulate the design of the irregular topology for the RIS, where topology matrix's N diagonal elements are set to 1 while the remaining diagonal elements, i.e., $N_s - N$, are assigned with value of 0. The constraints on phase shift, transmit power and topology design introduce high-dimensional and coupled variables into this non-convex problem, which makes it highly challenging to solve directly. As stated before, the method in [31] separates the optimization of RIS topology (via ATS) and precoding design (via NECE) that results in increased complexity due to sequential and separate optimization steps and a reliance on iteration numbers and neighbourhood size. In dense deployments, this approach struggles with convergence and may get stuck in local optima. We aim solving these problems while increasing system capacity simultaneously by employing PSO, which enables simultaneous optimization of the RIS topology $\mathbf{T}$, the beamforming $\mathbf{W}$ and the phase-shift $\mathbf{\Theta}$. PSO improves the WSR objective iteratively by updating each particle's local and global best solutions.

III. Proposed Algorithm

The proposed joint RIS topology and precoding design framework is presented in this section to avoid the local optimum and enhance the capacity of wireless networks. We first discuss standard PSO and then apply it to efficiently solve the optimization problem P1. Next, we introduce an improved PSO algorithm and exploit it for further improving the capacity of irregular RIS-aided wireless network.

A. Proposed Standard PSO for Simultaneous Optimization of RIS Topology and Precoding Design

PSO is a population-based optimization technique inspired by the collective social behaviours observed in nature, such as the flocking dynamics of birds. Due to its simplicity and effectiveness, PSO is particularly efficient in solving complex and non-convex optimization problems. In this method, a swarm of particles explore the solution space collaboratively to obtain optimal solutions. Each particle's position is adjusted by taking into account its best-known position and the positions of its neighbors, allowing for efficient exploration and exploitation of the search space. The standard PSO technique operates by initializing a population of particles, with each particle representing a potential solution in the form of topology configurations, beamforming vectors and RIS phase shifts in our case. Then, the position of each particle is updated based on their best-known position as well as the best-known position of the entire swarm, thereby improving the solution iteratively until convergence is achieved. Below are the main steps of PSO algorithm.

1. Initialization: Each particle $\mathbf{X}_i$ is randomly initialized within the defined bounds of the search space and represents a potential solution to the optimization problem:

$$\mathbf{X}_i = [x_{i,1}, x_{i,2}, \ldots, x_{i,d}], \tag{14}$$

where d is the dimension of the problem, i.e., the total number of variables or parameters that define a single solution. In addition, each particle has a personal best position $\mathbf{P}_i$ and associated velocity $\mathbf{V}_i$:

$$\mathbf{V}_i = [v_{i,1}, v_{i,2}, \ldots, v_{i,d}], \quad \mathbf{P}_i = \mathbf{X}_i. \tag{15}$$

$\mathbf{P}_i$ denotes the best position discovered by the i-th particle during its search process. Besides, each particle also maintains its global best position.

2. Iteration Process:

For each iteration i:

1) Evaluate the fitness of each particle in comparison to its best previous location using a fitness function $f(\mathbf{X}_i)$, which quantifies how well the solution satisfies the optimization criteria.
2) For each particle, the personal best position is compared and updated as:

$$\text{if } f(\mathbf{X}_i) > f(\mathbf{P}_i) \Rightarrow \mathbf{P}_i = \mathbf{X}_i. \tag{16}$$

3) update the global best by comparing the best fitness of all particles:

$$\text{if } f(\mathbf{X}_i) > f(\mathbf{G}) \Rightarrow \mathbf{G} = \mathbf{X}_i. \tag{17}$$

where $\mathbf{G}$ is the best position discovered by any particle within the swarm, which is determined by evaluating the fitness function for all particles and selecting the one with the highest fitness level.
4) Update each particle's velocity and position:

$$\mathbf{V}_i = w \cdot \mathbf{V}_i + c_1 \cdot r_1 \cdot (\mathbf{P}_i - \mathbf{X}_i) + c_2 \cdot r_2 \cdot (\mathbf{G} - \mathbf{X}_i), \tag{18}$$

$$\mathbf{X}_i = \mathbf{X}_i + \mathbf{V}_i, \tag{19}$$

where w denotes inertia weight which controls the effect of the previous velocity, c_1, represents cognitive coefficient, c_2 is social coefficient, and r_1, r_2 are random values uniformly distributed in $[0, 1]$. The velocity vector determines how much the position of particle will be changed in the next iteration and the acceleration coefficients impact the exploration of search space of the particle. Then, by adding the updated velocity to the current position, the new position is calculated.

3. Termination: Evaluate the level of fitness for each particle Until a specific stopping criterion is met, such as reaching a predefined maximum number of iterations or achieving a satisfactory performance.

Our aim is to maximize the WSR while simultaneously designing the RIS topology matrix $\mathbf{T}$, the beamforming vectors $\mathbf{w}_k$ and the RIS phase shifts $\mathbf{\Theta}$. We exploit standard PSO algorithm to enhance the overall capacity of multiuser communication system since it provides a natural framework because of its ability to handle multiple interrelated variables in a single optimization process.

Each particle $\mathbf{X}_i \in \mathbb{R}^d$, initialized randomly within defined bounds, represents a candidate solution in the optimization space. In our problem, the solution space consists of three key components RIS topology configurations, beamforming vectors, and RIS phase shifts. The representation of particle including all three components can be expressed as

$$\mathbf{X}_i = [\mathbf{T}_i, \mathbf{w}_i, \mathbf{\Theta}_i]. \tag{20}$$

Each particle explores the combined space of RIS topology, beamforming vectors and phase shifts by updating its positions, thereby efficiently searching for a configuration which maximizes the performance. The associated velocity $\mathbf{V}_i$ of each particle can be expressed as:

$$\mathbf{V}_i = [v_{i,1}, v_{i,2}, \ldots, v_{i,d}]^T. \tag{21}$$

The velocity vector determines how particle moves through the solution space. Additionally, each particle maintains its best-known position $\mathbf{P}_i$ and the global best position $\mathbf{G}$:

$$\mathbf{P}_i = \mathbf{X}_i, \quad \mathbf{G} = \arg\max_i f(\mathbf{X}_i), \tag{22}$$

where f is the fitness function based on the WSR. The personal best position, in the context of our optimization problem, reflects the best combination of irregular RIS topology (represented by the topology matrix $\mathbf{T}$) and precoding (represented by beamforming vectors and phase shits $\mathbf{\Theta}$). If the particle finds a configuration during exploration of search space that yields a higher WSR than its previously best recorded, this new configuration will be used for next step. Next step is evaluating the fitness of particles by using fitness function

$$f(\mathbf{X}_i) = \sum_{k=1}^{K} w_k \log_2 (1 + \text{SINR}_k). \tag{23}$$

This function quantitatively assesses how well the configuration of each particle performs in terms of maximizing the WSR by computing the SINR based on the current positions of the particles for each user. The subsequent steps, after assessing the fitness function for each particle, follow a similar procedure as previously discussed in the standard PSO method for updating the particle velocities and positions. Specifically, the velocity based upon its current velocity and the distance to its personal and global best positions are updated for each particle. The algorithm continues until a stopping criterion is met, such as achieving convergence or reaching predefined iterations.

B. An Improved PSO Algorithm for Simultaneous Optimization of RIS Topology and Precoding Design

Now we present the improved PSO algorithm that introduces dynamic parameters. The parameters in PSO can limit the local and global search capabilities of swarms and can have a significant effect on the accuracy of optimization. The parameters in the improved PSO are adjusted dynamically throughout the optimization process that improves the exploration and exploitation abilities of the algorithm and leads to enhanced performance in finding optimal solutions. The usage of dynamic parameters instead of static parameters offers substantial advantages. More balanced exploration and exploitation strategy can be achieved by adjusting cognitive and social coefficients and inertia weight throughout the optimization process. Static PSO parameters can often lead to premature convergence, where particles become stuck in local optima, which often results in suboptimal solutions. Dynamic parameters, in contrast, enable the PSO to adapt its search behaviour based upon the current optimization stage that facilitate a more efficient exploration of the solution space. Inertia weight is a key parameter that plays a vital role in balancing exploration and exploitation. Thus, we propose a novel parameter as follows:

$$w_{\text{novel}} = 1.2 - 0.5 \cdot \left(\frac{\text{iter}}{\text{max\_iter}} \right), \tag{24}$$

Algorithm 1 Improved PSO for Simultaneous Optimization of irregular RIS Topology and Precoding Design

Input:
Number of users K, antennas at BS M, SNR
Number of RIS elements N, grid points N_S
Channel matrices $\mathbf{H_d}$, $\mathbf{H_r}$, $\mathbf{G_S}$
PSO parameters: I_{max} (iterations), N_p (particles)
Initialize:
Initialize binary particle positions $\mathbf{T}_i \in \{0,1\}^{N_S}$ randomly
Initialize particle velocities $\mathbf{V}_i = \mathbf{0}^{N_S}$
Initialize $\mathbf{p}_{best,i} = \mathbf{T}_i$, $\mathbf{g}_{best}$, and their scores
for $iter = 1$ to I_{max} **do**
  Update Dynamic PSO Parameters:
  $w = 1.2 - 0.5 \cdot (iter/I_{max})$
  $c_1 = 2 + 0.5 \cdot (iter/I_{max})$
  $c_2 = 2 - 0.5 \cdot (iter/I_{max})$
  for each particle $i = 1$ to N_p **do**
    Enforce Topology Constraint:
    if $\sum \mathbf{T}_i > N$ **then**
      Randomly deactivate $(\sum \mathbf{T}_i - N)$ elements
    else if $\sum \mathbf{T}_i < N$ **then**
      Randomly activate $(N - \sum \mathbf{T}_i)$ elements
    end if
    Joint Optimization:
    Calculate effective channel $\mathbf{H}_{eff} = \mathbf{H_r}\text{diag}(\mathbf{T}_i)\mathbf{G_S}$
    Optimize precoding matrix $\mathbf{W}$ using ZF method
    Update precoding based on current topology
    Calculate SINR for each user with joint topology-precoding
    Compute WSR using updated SINR values
    Update Best Solutions:
    if $WSR > p\_best\_score_i$ **then**
      Update particle's best topology and precoding
      if $WSR > g\_best\_score$ **then**
        Update global best topology and precoding
      end if
    end if
  end for
  for each particle $i = 1$ to N_p **do**
    Generate random vectors $\mathbf{r_1}, \mathbf{r_2} \in [0,1]^{N_S}$
    Update Velocity:
    $\mathbf{V}_i \leftarrow w\mathbf{V}_i + c_1\mathbf{r_1} \odot (\mathbf{p}_{best,i} - \mathbf{T}_i) + c_2\mathbf{r_2} \odot (\mathbf{g}_{best} - \mathbf{T}_i)$
    Update Position:
    $\mathbf{T}_i \leftarrow \text{round}(\mathbf{T}_i + \mathbf{V}_i)$
    Update precoding based on new topology
  end for
end for
return Global best topology, precoding matrix, and achieved WSR

where $iter$ and $iter_{max}$ are the current iteration and maximum number of iterations, respectively. The proposed w_{novel} starts at a higher value that allows particles to explore wider search space. It decreases as iterations increase, ensuring that particles gradually focus on the most promising areas of the search space by reducing the impact of the previous velocity update on the current velocity update. This transition from a relatively higher to a lower value enables a good tradeoff between exploration and exploitation, helping to escape the local optimum and converge more effectively towards the global optimum.

To further enhance the capabilities of standard PSO, we introduce new cognitive and social coefficients $c_{1,\text{novel}}$ and $c_{2,\text{novel}}$ defined as

$$c_{1,\text{novel}} = 2 + 0.5 \cdot \left(\frac{\text{iter}}{\text{max\_iter}}\right), \tag{25}$$

$$c_{2,\text{novel}} = 2 - 0.5 \cdot \left(\frac{\text{iter}}{\text{max\_iter}}\right). \tag{26}$$

It can be observed that, similar to w_{novel}, $c_{1,\text{novel}}$ and $c_{2,\text{novel}}$ are also adjusted during the iteration routine. The performance of the improved PSO is robust to small variations in w_{novel}, $c_{1,\text{novel}}$ and $c_{2,\text{novel}}$. The velocity update equation, based on the novel parameters, can be expressed as

$$\begin{aligned}\mathbf{V}_i = w_{\text{novel}} \cdot \mathbf{V}_i + c_{1,\text{novel}} \cdot r_1 \cdot (\mathbf{P}_i - \mathbf{X}_i) \\ + c_{2,\text{novel}} \cdot r_2 \cdot (\mathbf{G} - \mathbf{X}_i).\end{aligned} \tag{27}$$

Note from velocity update equation that the cognitive parameter have greater effect on enhancing convergence towards individual optimal solutions. The contribution of personal best positions grows with a higher $c_{1,\text{novel}}$ as can be observed from following part of velocity update equation

$$\text{Influence of cognitive term} = c_{1,\text{novel}} \cdot r_1 \cdot (\mathbf{P}_i - \mathbf{X}_i). \tag{28}$$

The parameter $c_{1,\text{novel}}$ increases with growing iterations that helps to refine the search based on past experiences, improving the particles ability to locate its best-known position. Therefore, the new cognitive coefficient encourages the particles to exploit search areas which have provided better results, promoting better refinement of individual particle locations with the increasing number of iterations. Similarly,

$$\text{Influence of social term} = c_{2,\text{novel}} \cdot r_2 \cdot (\mathbf{G} - \mathbf{X}_i), \tag{29}$$

indicates the optimal location of the population and the cognitive capacity of particle to locate this place is determined by $c_{2,\text{novel}}$. The decreasing value of cognitive parameter with increasing iteration count reduces the effect of global best solutions over time, allowing particles to focus more on their local. This tradeoff is important to avoid premature convergence to suboptimal solutions and let particles to look for other promising parts of the search space. The combination of dynamically adjusted inertial weight, cognitive and social parameters contributes significantly to the ability of PSO algorithm to adapt to the changing characteristics of the optimization problem.

In summary, the inertia weight w_{novel} is larger at the initial phase, allowing particles to explore the search space more

freely. The cognitive and social coefficients encourage particles to explore new regions since they are smaller during the initial iterations that lessens the influence of past experiences and the global best. The inertia weight decreases as the algorithm progresses, which reduce the exploration and focus the movement of particles on the most promising regions around the current best solutions. At the same time, the cognitive coefficient c_1 reinforces the influence of the own experience of the particles as it increases, while the social coefficient c_2 reduces the influence of the global best as it decreases. This assists particles for refining their positions in the optimal region. The generalized pseudo algorithm of the improved PSO is given in Algorithm 1 and its brief explanation is detailed as follows. The necessary parameters such as the dimension of the optimization problem, the objective function, and the problem constraints are initialized first. Following that, the algorithm randomly initializes particle positions within the search space and setting their initial velocities to zero, establishing the particle swarm.

Based on these initial positions, the personal best position of each particle, denoted as $\mathbf{p}_{\text{best},i} \in \{0,1\}^{N_s}$, and the global best position, denoted as $\mathbf{g}_{\text{best}} \in \{0,1\}^{N_s}$, are initialized. The vector $\mathbf{p}_{\text{best},i}$ represents the best topology configuration found by particle i throughout the optimization process, corresponding to the highest WSR it has achieved. In contrast, $\mathbf{g}_{\text{best}}$ represents the best topology configuration identified by any particle in the entire swarm, corresponding to the highest WSR found globally up to the current iteration. The main iteration loop of the algorithm begins by updating its dynamic control parameters. These parameters are adjusted based on the current iteration number. The process then uses any problem-specific constraints and evaluates the fitness of each particle in the swarm using the objective function. If a particle i finds a configuration with WSR better than its previous personal best, the personal best $\mathbf{p}_{\text{best},i}$ is updated. Similarly, the global best $\mathbf{g}_{\text{best}}$ is also updated if this new personal best is better than the global best. After all particles are evaluated, the velocity and positions of all particles are updated. Velocity determines the direction and magnitude of topology changes and there are three components to the velocity update: the inertial component using w, the cognitive and social component based on $c1, c2$, respectively. The position is then updated using this new velocity. Here, the round operation converts the continuous velocity updates to binary topology decisions. After updating particle positions with $\mathbf{T}_i \leftarrow \text{round}(\mathbf{T}_i + \mathbf{V}_i)$, the resulting values are real numbers. The Round () operation maps these to binary values: $\mathbf{T}_i \leftarrow \text{round}(\mathbf{T}_i + \mathbf{V}_i)$, where $\text{round}(x) = 1$ if $x \geq 0.5$, and $\text{round}(x) = 0$ if $x < 0.5$. This is followed by our constraint enforcement mechanism that ensures exactly N elements are active by randomly adjusting elements. This whole process continues until the maximum number of iterations is reached, where the algorithm returns the global best solution and its corresponding fitness value.

The improved PSO can be applied to numerous optimization problems, where search space is large and non-convex, and problem involves balancing exploration and exploitation. Such as multi-objective optimization where multiple conflicting objectives need to be optimized, and in machine learning where tuning hyperparameters often needs a better tradeoff between exploration of the hyperparameter space and exploitation of known good configurations. In this paper, similarly to the standard PSO Algorithm, we apply the introduced improved PSO for solving the formulated joint optimization problem to showcase the effectiveness of the algorithm. As a result of new dynamic parameters that allow for a flexible search strategy, the improved PSO obtains much better results compared to standard PSO. Numerical results in the results section illustrate that the implementation of improved PSO can greatly improve convergence and enhance the capacity of wireless networks.

IV. Validation and Analysis of improved PSO

A. Validation

We validate the improved PSO technique by testing it over a complex multi-modal Michalewicz benchmark function, which is a widely used test function for evaluating optimization techniques. The benchmark is chosen due to its complexity, with multiple local optima, which makes it an ideal candidate to evaluate the ability of optimization methods to find the global minimum. Performance of standard and improved PSO in terms of the time taken for convergence and the global minimum approximation are considered. The tests are carried out in 2D and 5D space. The equation of the function is

$$f(\mathbf{x}) = -\sum_{i=1}^{n} \sin(x_i) \left(\sin\left(\frac{i x_i^2}{\pi} \right) \right)^{2m}. \tag{30}$$

We consider 30 particles, 200 maximum iterations, and $[0, \pi]$ search space for testing. The 3D plots (figure 2 and 3) illustrate the optimization performance of both standard PSO and improved PSO algorithms on the Michalewicz function. As can be observed, multiple local minima are present in both plots, making it difficult to locate the global minimum for optimization algorithms. Both algorithms attempt to find the global minimum that is represented by the deepest point (dark blue region) as in Figure 1. indicating both algorithms successfully found the approximate region of the global minimum. The standard and improved PSO global minima are marked by blue and red dots, respectively, at the lowest point of the surface, demonstrating that both approaches successfully located the approximate region of the global minimum. A different perspective of the same optimization problem for 5D space is shown in Figure 2, where the global minimum points clearly marked below the surface. This figure also shows that the both algorithms successfully found the approximate region of the global minimum. While the surface plots provide qualitative insights into the behavior of the algorithms, next we provide a quantitative evaluation.

Table I compares expected global minimums, which is benchmark value of Michalewicz function, and obtained global minimums for both the standard and the improved PSO using 2D and 5D space. It can be seen that the improved PSO is capable of obtaining global minimum values that match the expected values across both dimensions. Specifically, the global minimum obtained in 2D space for improved PSO is -1.801254, just a slight deviation from the expected value of -1.8013. Similarly, the obtained global minimum for improved

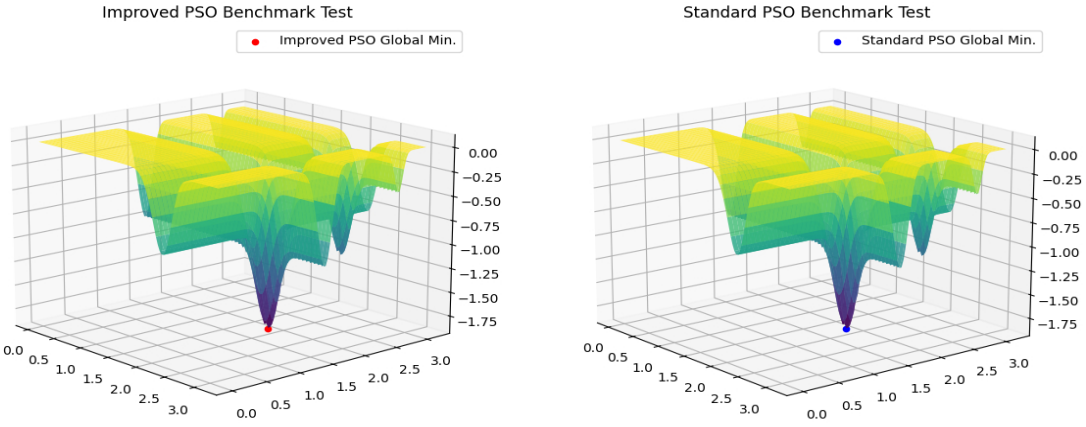

Fig. 2. Michalewicz function plot in 2D for standard and improved PSO methods

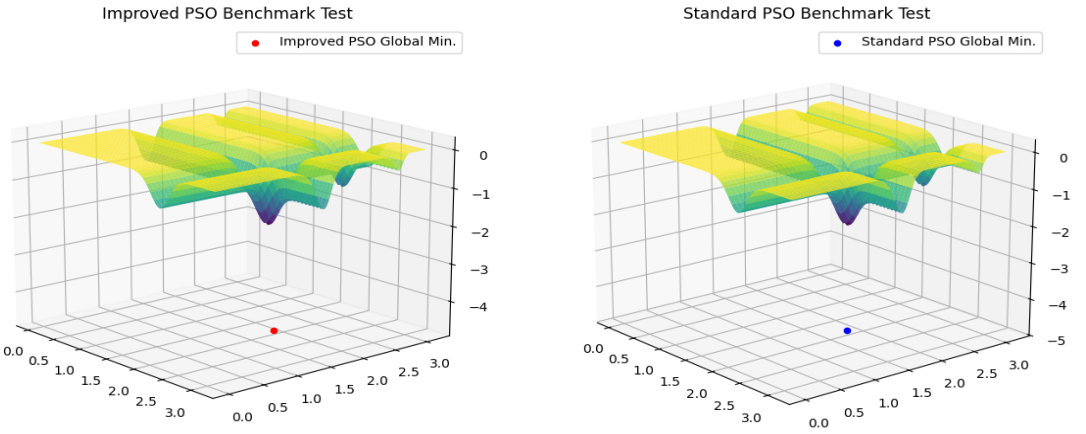

Fig. 3. Michalewicz function plot in 5D for standard and improved PSO methods

Algorithm	Dimension	Expected Global Minimum	Obtained Global Minimum	Difference
Standard PSO	2D	-1.8013	-1.801303	0.000003
	5D	-4.687658	-4.678658	0.009000
improved PSO	2D	-1.8013	-1.801254	0.000046
	5D	-4.687658	-4.687586	0.000072

TABLE I
EXPECTED AND OBTAINED RESULTS FOR MICHALEWICZ FUNCTION FOR STANDARD AND IMPROVED PSO

Algorithm	Dimension	Time Taken for Convergence (seconds)	Iterations
Standard PSO	2D	0.3477	126
	5D	0.8131	175
improved PSO	2D	0.1523	73
	5D	0.7804	118

TABLE II
TIME TAKEN FOR CONVERGENCE FOR STANDARD AND IMPROVED PSO

PSO in the 5D case is -4.687586, which is very close to the expected value of -4.687658. It can be further seen from the table that the standard PSO also deviates by a small margin for 2D but it has a larger deviation for 5D compared to the improved PSO. This suggests that, compared to standard PSO, the improved PSO consistently delivers more accurate global minimum approximations, particularly in higher-dimensional spaces. Next we compare the time taken for convergence, an important metric to assess the efficacy of optimization techniques. It can be noted from Table II that the improved PSO takes only 0.1523 seconds compared to 0.3477 seconds for standard PSO to converge. While the time difference is less in case of 5D space but improved PSO still takes less time to converge compared to standard PSO. It can be noted from Table II that, for 2D space, the standard PSO took 126 iterations while improved PSO took 73 iterations, and for 5D space improved PSO took 118 iterations while standard PSO took 175 iterations for convergence. Thus, it can be concluded that the improved PSO achieves extremely closer approximations to the expected global minimum and does so in a shorter time and less iterations. This makes it a highly reliable and efficient optimization tool for complex multi-variable optimization problems. It is worth mentioning that these test are carried out on a system having Intel core i5-9500K CPU using 16GB RAM. In addition, we remark that the improved PSO algorithm can also be extended to N-dimensional space.

B. Convergence Analysis of improved PSO

We provide the convergence analysis of the PSO in order to show that the dynamic adjustment of the parameters leads to convergence towards an optimal solution, whereas achieving the better tradeoff between exploration and exploitation phases of the search. Rigorous analysis based on bounded convergence and its Lyapunov stability is presented in order to guarantee convergence. Mathematical justification for why dynamic parameters prevent over-exploration and significantly enhance the convergence speed is also provided.

The idea of bounded convergence refers to the fact that the velocities and positions of particles constrained within the specified bounds throughout the optimization process. This ensures that, as the iteration progress, the algorithm does not diverge or make extremely larger steps, which can lead to instability. The bounded nature of PSO ensures that the particles ultimately converge to a stable region of the search space, thus guaranteeing convergence of the algorithm.

In our case, the velocity update equation has a dynamic inertia weight $w(t)$, cognitive coefficient $c_1(t)$, and social coefficient $c_2(t$, and can be defined by

$$\begin{aligned}\mathbf{V}_i(t+1) = w(t)\cdot\mathbf{V}_i(t) + c_1(t)\cdot r_1\cdot(\mathbf{P}_i - \mathbf{X}_i(t)) \\ + c_2(t)\cdot r_2\cdot(\mathbf{G} - \mathbf{X}_i(t)),\end{aligned} \tag{31}$$

where $\mathbf{V}_i^{(t+1)}$ and $\mathbf{X}_i^{(t)}$ are the new velocity and the position at iteration t of particle i, respectively. The position update with dynamic velocity is given by

$$\mathbf{X}_i(t+1) = \mathbf{X}_i(t) + \mathbf{V}_i(t+1). \tag{32}$$

We can observe that with increasing number of iterations, the velocity of particles decreases as the value of inertia weight decreases and the cognitive and social parameters increase, leading to a more precise search around the optimal region. In the convergence analysis of PSO algorithms, the concept of constraining the velocity and position is commonly used. Assume that the velocity and position updates are bounded by the problem constraints, which ensures that particles do not leave the search space. Thus, to prevent instability, we can impose velocity and position bounds as

$$|\mathbf{V}_i(t)| \le \mathbf{V}_{\max}, \quad |\mathbf{X}_i(t)| \le \mathbf{X}_{\max}, \tag{33}$$

where $\mathbf{V}_{max}$ and $\mathbf{X}_{max}$ denote the maximum allowable velocities positions, respectively. The velocity constraints enable the particles from making extremely larger steps since that could lead to overshooting or instability, whereas the position bounds guarantee that particles remain within the feasible search area. The inertia weight $w(t)$ decreases As the algorithm progresses allowing the particles to make smaller adjustments to their positions, which ensures convergence towards the optimal solution. The bounded updates control this behavior, resulting in monotonically decreasing Lyapunov function, which confirms that the algorithm converges to a desired solution. Lyapunov function is a powerful concept used to analyze the stability of dynamical systems. We can use direct Lyapunov method in the context of PSO to establish that it converges to a stable point. The idea is to define a Lyapunov function that is a scalar function, which decreases monotonically over time as the particles move towards the optimal solution. We define the Lyapunov function $V(\mathbf{X}_i)$ as the negative of fitness function in our case

$$V(\mathbf{X}_i) = -f(\mathbf{X}_i) = -\sum_{k=1}^{K}\alpha_k \log_2\left(1 + SINR_k\right). \tag{34}$$

$V(\mathbf{X}_i) = -f(\mathbf{X}_i)$ serves as a potential function where $\Delta V(\mathbf{X}_i) < 0$ guarantees monotonic WSR improvement. This aligns with discrete-time Lyapunov stability theory, ensuring the swarm converges to local maxima of $f(\mathbf{X}_i)$.

In order to prove the convergence, we need to show that, with each iteration, the function $V(\mathbf{X}_i)$ is decreasing.

$$\frac{dV(\mathbf{X}_i)}{dt} \le 0.$$

This condition shows that the fitness function does not indefinitely increase but it stabilizes, which indicates that the convergence of particles to a stable region of the search space.

The dynamic nature of the parameters inertia weight $w(t)$, cognitive $c_1(t)$ and social $c_2(t)$ coefficients are key to the fast convergence of the improved PSO algorithm. These parameters provide good tradeoff between exploration and exploitation phases throughout optimization, enhancing both the accuracy and the speed of convergence. The inertia weight $w(t)$ decreases over time as explained earlier:

$$w(t) = w_{\max} - (w_{\max} - w_{\min})\,\frac{t}{T}. \tag{35}$$

Similarly, the cognitive coefficient increases and the social coefficient decreases over time as shown below

$$c_1(t) = c_{\min} + (c_{\max} - c_{\min})\frac{t}{T}, \tag{36}$$

$$c_2(t) = c_{\max} - (c_{\max} - c_{\min})\frac{t}{T}. \tag{37}$$

This strategy allows the particles to adapt their search strategy over time, improving overall performance. Moreover, the exploitation-exploration tradeoff is managed efficiently since the algorithm adapting its behavior as the optimization progresses. To further analyze impact of dynamic parameters on convergence of algorithm, we can express the Lyapunov function $V(\mathbf{X}_i)$ and its variation during the optimization process. The change in the Lyapunov function $\Delta V(\mathbf{X}_i)$ at each iteration t can be expressed by

$$\Delta V(\mathbf{X}_i) = V(\mathbf{X}_i(t)) - V(\mathbf{X}_i(t-1)) \tag{38}$$

$$= -\left(f(\mathbf{X}_i(t)) - f(\mathbf{X}_i(t-1))\right). \tag{39}$$

Then by substituting the fitness function in above equation, we get:

$$\Delta V(\mathbf{X}_i) = -\sum_{k=1}^{K} \alpha_k \log_2\left(1+\gamma_k(t)\right) + \sum_{k=1}^{K} \alpha_k \log_2\left(1+\gamma_k(t-1)\right). \tag{40}$$

While the velocity update equation depends on the previous velocity and the distance to the personal and global best positions, it guarantees that as the algorithm progresses the particles move in a direction that improves the fitness function, which leads to a decrease in $\Delta V(\mathbf{X}_i)$.

Therefore, we have:

$$\Delta V(\mathbf{X}_i) < 0, \tag{41}$$

which shows that, with each iteration, the Lyapunov function decreases that confirms the system is stabilizing and converging toward an optimal solution.

C. Complexity Analysis

We present a quantitative complexity analysis and comparison of the ATNE and the PSO methods, for the problem of RIS topology and precoding design in multi-user MIMO wireless systems. The maximum number of required searches for each approach is used as the primary complexity metric. First, we discuss the complexity of PSO technique that jointly optimizes both RIS topology and precoding design in a single framework. Then, the complexity of the conventional alternative optimization based method is discussed.

The searching complexity of PSO is determined by the number of particles P in the swarm, the number of maximum iterations I_{max} until convergence, the number of active RIS elements or grid points N_s, and the number of users K. For each particle in every iteration, the algorithm evaluates topology configurations and computes the WSR for K users. Therefore, the searching complexity of the PSO algorithm in terms of evaluations is

$$C_{\text{PSO}} = P \times I_{max} \times N_s \times K, \tag{42}$$

where P particles explore the solution space over I_{max} iterations, evaluating N_s grid points for K users. PSO efficiently explores the solution space through guided particle movements, making it computationally feasible for large systems.

In contrast to PSO, ATNE method decouples the topology and precoding designs, and optimize them separately. In ATNE, the ATS algorithm evaluates the candidate configurations for each configuration. The total number of searches for ATS, depending on the number of iterations I_T and the neighborhood size Q, can be defined by

$$C_{\text{ATS}} = Q \times I_T. \tag{43}$$

Once the topology configuration is fixed, the NECE technique is utilized for precoding optimization. NECE searches through I_N iterations, testing C primary candidates and $N(2^b-1)$ extra candidates for a given specific topology. Therefore, its complexity is given by

$$C_{\text{NECE}} = I_N \times (C + N(2^b - 1)). \tag{44}$$

The overall complexity for ATNE algorithm that combines ATS and NECE is thus

$$C_{\text{ATNE}} = Q \times I_T \times I_N \times (C + N(2^b - 1)). \tag{45}$$

We can observe from (42) and (45) that the searching complexity of both the proposed PSO and the conventional method grows linearly with the growing system size. However, proposed PSO algorithm has significantly lower complexity compared to the conventional scheme since $P \times I_{max}$ is typically much smaller than $Q \times I_T \times I_N$ in practical implementations. Moreover, while ATNE requires $(C+N(2^b-1))$ additional evaluations for precoding optimization, PSO inherently handles both topology and precoding optimization in each iteration. The complexity of PSO remains manageable even with increasing grid points as it does not require to evaluate all possible combinations. In addition, the parallel nature of PSO allows for efficient hardware implementation.

V. Numerical Results

We provide numerical results in this section to validate the effectiveness of the introduced PSO methods in RIS-assisted wireless network. A multiuser moderate MIMO communication system is considered where BS with M antennas is the center point, i. e., it is located at (0 , 0) and simultaneously serve K users with single-antenna that are randomly and uniformly scattered in a circular area centred at (50 m, 0 m). It is assumed that the communication between BS and users is assisted by irregular RIS situated at (50 m, 5 m). Irregular RIS has N elements dispersed across a rectangular area with N_s grid points. We generate the coefficients of the channel according to the channel model discussed in Section II, and we consider the perfect channel state information to evaluate the performance of all algorithms. The parameters are set to $\omega_{BR} = 0$, $\omega_{BU} = 0$, $\omega_{RU} = 1$, $\beta_{BR} = 3.5$, $\beta_{RU} = 2$, $\beta_{BU} = 4$, $C_d = -30$ dB and $C_r = -60$ dB. We use the

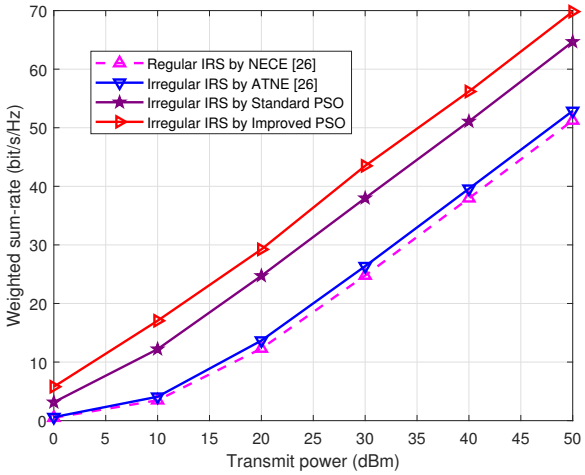

Fig. 4. WSR performance versus transmit power for a system with $M = K = 4$, $N = 16$ and 32 grid points N_s.

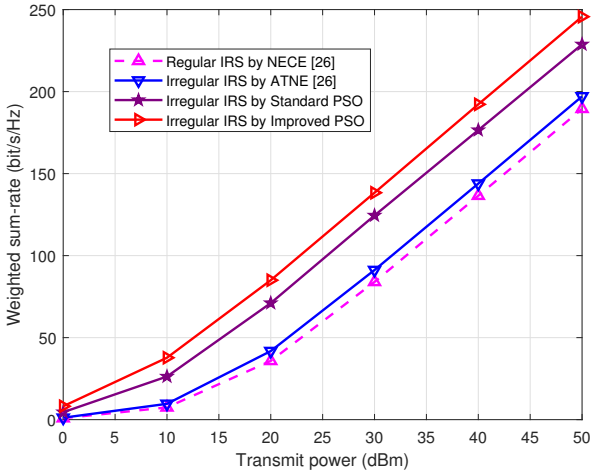

Fig. 5. WSR as a function of transmit power for a RIS-assisted MIMO system having $M = K = 16$, $N = 32$, $N_s = 64$.

proposed standard and improved PSO to solve the formulated problem in order to simultaneously obtain the irregular RIS topology and precoding design. The number of iterations and particles for proposed PSO algorithms are set to $I_{max} = 8$, $N_p = 10$, respectively. The WSR performance of the proposed algorithms is compared with conventional ATNE method [31] where the ATS technique is utilized to obtain the irregular topology and NECE is used for precoding design, and the parameters of the ATNE are same as in [31]. As a benchmark, the precoding optimization for the conventional regular RIS-assisted system [39] based upon the NECE scheme is included.

Figure 4 compares the WSR performance versus transmit power, considering the system with 4 antennas at the BS and 4 users. The 16 RIS elements with 32 grid points assists in providing a high-quality link between the BS and users. The conventional method with irregular RIS slightly performs better than the baseline regular RIS but the performance improvement is not significant. However, it can be observed that the proposed standard PSO algorithm significantly outperforms both the baseline and ATNE with irregular RIS system with a limited number of RIS elements. The performance difference between the proposed standard PSO and baseline is 10.01 dBm and between ATNE and baseline is 1.228 dBm. Note, further, that the improved PSO achieves excellent performance compared to all other methods including proposed standard PSO. Thus, we can say that the proposed PSO algorithms can greatly enhance the capacity of irregular RIS-based wireless system for a considered setup.

Figure 5 illustrates the WSR performance as a function of transmit power for a larger system scenario with 16 BS antennas and 16 users. We consider 32 RIS elements with 64 grid points in this simulation. Results exhibit a similar trend as in Fig. 4 demonstrating that the irregular RIS with the conventional method slightly improved over the baseline regular RIS. Nonetheless, this improvement remains marginal, which suggests that even though irregular RIS has the potential to enhance the performance of the system by offering more flexible configurations, the conventional optimization approaches do not fully capture these benefits. Notably, the proposed standard and improved PSO algorithms achieve considerable performance gains over both the ATNE-based irregular RIS and baseline methods. This is mainly due to that the ATS method rely on a relatively simple topology selection strategy, which may not effectively exploit the available degrees of freedom in the system and NECE requires more number of iterations to achieve desired precoding results. The PSO approaches, in contrast, are more robust in exploring the solution space, which allows them to optimize the irregular RIS configurations better and obtain more significant performance improvements.

Figure 6 compares the WSR performance against transmit power for MIMO system with 32 antennas at the BS and 16 users, considering 64 RIS elements with 128 grid points. The system in this higher configuration exhibits increased complexity, which provides a more diverse propagation environment and better opportunities for optimization. Observe that the performance difference between the irregular RIS topology with ATNE and the conventional regular RIS becomes negligible in this case. This implies that the conventional joint optimization approach is not capable in effectively exploiting the spatial diversity benefits provided by the irregular RIS, resulting in degraded performance. The key observation, however, is that the proposed PSO-based optimization algorithms continue to exhibit significant performance gains over the conventional approach, highlighting the superior capability of the proposed optimization strategy in exploiting the increased degrees of freedom in the system. The PSO methods are particularly effective in navigating the larger solution space, optimizing the RIS configuration more efficiently than the conventional methods. In summary, with the larger system configuration, the performance of irregular RIS with the conventional optimization approach and regular RIS becomes the same, however, the proposed PSO algorithms maintain a substantial advantage. This emphasizes that the proposed PSO-based optimization approaches can fully leverage the potential of large-scale RIS-assisted systems

The Figure 7 shows the relationship between the WSR

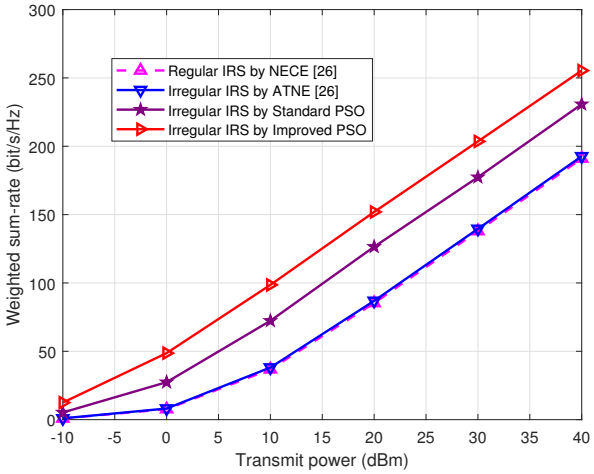

Fig. 6. WSR performance comparison against transmit power for a RIS-assisted moderate MIMO system. $M = 32$, $K = 16$, $N = 64$, $N_s = 128$.

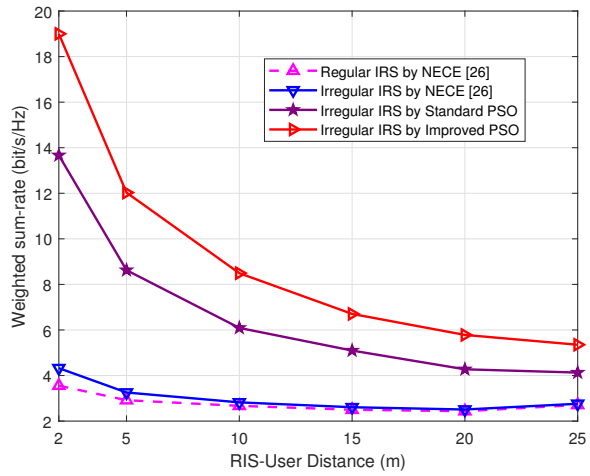

Fig. 7. WSR performance as a function of user distance across different optimization algorithms for a system with $M = 4$, $K = 4$, $N = 8$, $N_s = 16$.

and the distance between the RIS and users in a system with 4 antennas at the BS and 4 users. We consider 8 RIS elements with 16 gird points and provide the results for various distances ranging from 2 to 25 meters, which provides insights into system performance across typical outdoor and indoor deployment scenarios. It can be noted from figure that the WSR consistently decreases with the increasing RIS-user distance for all optimization approaches due to the increased path loss and signal attenuation at larger distances. The standard PSO-based irregular RIS maintains its advantages over conventional regular and irregular ATNE-based methods. The improved PSO based optimization technique exhibits superior performance across the entire distance range compared to other optimization techniques, suggesting that the adaptive optimization strategy in improved PSO is particularly effective at maintaining performance of the system under challenging long-distance scenarios. These finding indicate that improved PSO algorithm is suitable for scenarios that require longer

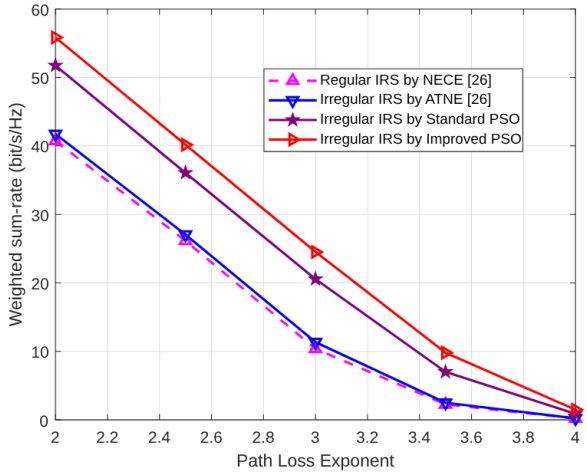

Fig. 8. WSR versus Path Loss Exponent. $M = 4$, $K = 4$, $N = 8$, $N_s = 16$.

communication distances.

Figure 8 shows the WSR performance as a function of path loss exponent across different RIS optimization schemes for a MIMO system with $M = K = 4$. We consider 8 RIS elements with 16 gird points, and transmit and noise power are set to 10 dBm and -90 dBm, respectively. The results are provided for varying path loss exponent values ranging from 2 to 4 that represents different propagation environments, lower values indicate free-space like conditions while higher ones indicate more severe attenuation of the signal. As the path loss exponent increases, all approaches exhibit a monotonic decrease in WSR, which is expected because of the stronger signal attenuation in more challenging propagation environments. Observe that, at lower path loss exponents, the regular RIS exhibits relatively better performance but as the environment becomes more challenging it experiences more pronounced degradation. In contrast, the irregular RIS with different algorithms outperform the regular RIS. We can see that the proposed both standard and improved PSO shows superior performance compared to irregular RIS based ATNE method. particularly the improved PSO algorithm consistently outperforms all algorithms across all path loss scenarios. A key factor to this superior performance is its adaptive optimization strategy throughout the iteration process, allowing it to better cope with varying channel conditions. Thus, the introduced improved PSO-based irregular RIS system can be more suitable for urban environments or indoor setups where typically higher path loss exponents are encountered.

VI. Conclusion

In this work, we enhanced the capacity of wireless communication system by exploiting irregular RIS. We have introduced new optimization techniques and applied them to address the joint problem of irregular RIS topology and precoding design. Specifically, the standard PSO scheme was proposed firstly and applied to the considered optimization problem. Based on this, we have introduced an improved variant of the PSO to further enhance convergence and computational efficiency. It has been shown that the proposed algorithms

significantly enhanced the system capacity by jointly optimizing the irregular RIS topology and precoding design within a single framework. The improved PSO has been validated through Michalewicz benchmark test for different dimensional spaces. Its complexity, convergence analysis and the impact of dynamic parameters on the convergence have been also discussed to further validate the improved PSO. Numerical results confirmed the benefits of the proposed algorithms, demonstrating the improved PSO outperformed standard PSO and significantly outperformed conventional methods. Additionally, we have highlighted the broader applicability of the improved PSO to other multi-variable optimization problems, highlighting its versatility and potential to advance various optimization challenges.

REFERENCES

[1] C. Pan and *et al.*, "Reconfigurable intelligent surfaces for 6g systems: Principles, applications, and research directions," *IEEE Commun. Mag.*, vol. 59, no. 6, pp. 14–20, 2021.

[2] F. Tariq, M. R. A. Khandaker, K.-K. Wong, M. A. Imran, M. Bennis, and M. Debbah, "A speculative study on 6g," *IEEE Wireless Commun.*, vol. 27, no. 4, pp. 118–125, 2020.

[3] W. Saad, M. Bennis, and M. Chen, "A vision of 6g wireless systems: Applications, trends, technologies, and open research problems," *IEEE Network*, vol. 34, no. 3, pp. 134–142, 2020.

[4] N. Rajatheva and *et al.*, "Scoring the terabit/s goal: Broadband connectivity in 6g," *arXiv preprint arXiv:2008.07220*, 2020.

[5] M. A. ElMossallamy, H. Zhang, L. Song, K. G. Seddik, Z. Han, and G. Y. Li, "Reconfigurable intelligent surfaces for wireless communications: Principles, challenges, and opportunities," *IEEE Trans. Cogn. Commun. Netw.*, vol. 6, no. 3, pp. 990–1002, 2020.

[6] Q. Wu and R. Zhang, "Towards smart and reconfigurable environment: Intelligent reflecting surface aided wireless network," *IEEE Commun. Mag.*, vol. 58, no. 1, pp. 106–112, 2020.

[7] M. Di Renzo and *et al.*, "Smart radio environments empowered by reconfigurable intelligent surfaces: How it works, state of research, and the road ahead," *IEEE J. Sel. Areas Commun.*, vol. 38, no. 11, pp. 2450–2525, 2020.

[8] C. Pan and *et al.*, "Multicell mimo communications relying on intelligent reflecting surfaces," *IEEE Trans. Wirel. Commun.*, vol. 19, no. 8, pp. 5218–5233, 2020.

[9] L. Liang and *et al.*, "Anomalous terahertz reflection and scattering by flexible and conformal coding metamaterials," *Adv. Opt. Mater.*, vol. 3, no. 10, pp. 1374–1380, 2015.

[10] J. Mirza and B. Ali, "Channel estimation method and phase shift design for reconfigurable intelligent surface assisted mimo networks," *IEEE Trans. Cogn. Commun. Netw.*, vol. 7, no. 2, pp. 441–451, 2021.

[11] E. Björnson and L. Sanguinetti, "Power scaling laws and near-field behaviors of massive mimo and intelligent reflecting surfaces," *IEEE Open J. Commun. Soc.*, vol. 1, pp. 1306–1324, 2020.

[12] T. J. Cui, M. Q. Qi, X. Wan, J. Zhao, and Q. Cheng, "Coding metamaterials, digital metamaterials and programmable metamaterials," *Light Sci. Appl.*, vol. 3, no. 10, p. 1218, 2014.

[13] Y. Liu and *et al.*, "Reconfigurable intelligent surfaces: Principles and opportunities," *IEEE Commun. Sur. Tut.*, vol. 23, no. 3, pp. 1546–1577, 2021.

[14] Y. Han, W. Tang, S. Jin, C.-K. Wen, and X. Ma, "Large intelligent surface-assisted wireless communication exploiting statistical csi," *IEEE Trans. Veh. Technol*, vol. 68, no. 8, pp. 8238–8242, 2019.

[15] Q. Wu and R. Zhang, "Intelligent reflecting surface enhanced wireless network via joint active and passive beamforming," *IEEE Trans. Wirel. Commun.*, vol. 18, no. 11, pp. 5394–5409, 2019.

[16] S. Zhou, W. Xu, K. Wang, M. Di Renzo, and M.-S. Alouini, "Spectral and energy efficiency of irs-assisted miso communication with hardware impairments," *IEEE Wirel. Commun. Lett.*, vol. 9, no. 9, pp. 1366–1369, 2020.

[17] G. Zhou, C. Pan, H. Ren, K. Wang, M. Elkashlan, and M. D. Renzo, "Stochastic learning-based robust beamforming design for ris-aided millimeter-wave systems in the presence of random blockages," *IEEE Trans. Veh. Technol*, vol. 70, no. 1, pp. 1057–1061, 2021.

[18] J. Zhang, X. Hu, and C. Zhong, "Phase calibration for intelligent reflecting surfaces assisted millimeter wave communications," *IEEE Trans. .Sig. Proces.*, vol. 70, pp. 1026–1040, 2022.

[19] S. Zhang and R. Zhang, "Capacity characterization for intelligent reflecting surface aided mimo communication," *IEEE J. Sel. Areas Commun.*, vol. 38, no. 8, pp. 1823–1838, 2020.

[20] C. Pan and *et al.*, "Multicell mimo communications relying on intelligent reflecting surfaces," *IEEE Trans. Wirel. Commun.*, vol. 19, no. 8, pp. 5218–5233, 2020.

[21] J. Wang, H. Wang, Y. Han, S. Jin, and X. Li, "Joint transmit beamforming and phase shift design for reconfigurable intelligent surface assisted mimo systems," *IEEE Trans. Cogn. Commun. Netw.*, vol. 7, no. 2, pp. 354–368, 2021.

[22] L. You, J. Xiong, Y. Huang, D. W. K. Ng, C. Pan, W. Wang, and X. Gao, "Reconfigurable intelligent surfaces-assisted multiuser mimo uplink transmission with partial csi," *IEEE Trans. Wirel. Commun.*, vol. 20, no. 9, pp. 5613–5627, 2021.

[23] Q. N. Le, V.-D. Nguyen, O. A. Dobre, and R. Zhao, "Energy efficiency maximization in ris-aided cell-free network with limited backhaul," *IEEE Commun. Lett.*, vol. 25, no. 6, pp. 1974–1978, 2021.

[24] L. You, J. Xiong, D. W. K. Ng, C. Yuen, W. Wang, and X. Gao, "Energy efficiency and spectral efficiency tradeoff in ris-aided multiuser mimo uplink transmission," *IEEE Trans. Sig. Proces.*, vol. 69, pp. 1407–1421, 2021.

[25] Z. Chen, J. Tang, X. Y. Zhang, Q. Wu, G. Chen, and K.-K. Wong, "Robust hybrid beamforming design for multi-ris assisted mimo system with imperfect csi," *IEEE Trans. Wirel. Commun.*, vol. 22, no. 6, pp. 3913–3926, 2023.

[26] M. Misbah, Z. Kaleem, W. Khalid, C. Yuen, and A. Jamalipour, "Phase and 3-d placement optimization for rate enhancement in ris-assisted uav networks," *IEEE Wireless Communications Letters*, vol. 12, no. 7, pp. 1135–1138, 2023.

[27] S. Kumar, J. K. Rai, P. Ranjan, and R. Chowdhury, "Secured and energy efficient wireless system using reconfigurable intelligent surface and pso algorithm," in *2024 IEEE International Conference on Interdisciplinary Approaches in Technology and Management for Social Innovation (IATMSI)*, vol. 2, 2024, pp. 1–5.

[28] V. D. Pegorara Souto, R. Demo Souza, and B. F. Uchôa-Filho, "Pso-based optimization of star-ris aided noma wireless communication networks," in *2024 19th International Symposium on Wireless Communication Systems (ISWCS)*, 2024, pp. 1–6.

[29] F. Tan, X. Xu, H. Chen, and S. Li, "Energy-efficient beamforming optimization for miso communication based on reconfigurable intelligent surface," *Physical Communication*, vol. 57, p. 101996, 2023. [Online]. Available: https://www.sciencedirect.com/science/article/pii/S1874490722002737

[30] M. Z. Siddiqi, T. Mir, M. Hao, and R. MacKenzie, "Low-complexity joint active and passive beamforming for ris-aided mimo systems," *Electronics Letters*, vol. 57, no. 9, pp. 384–386, 2021. [Online]. Available: https://ietresearch.onlinelibrary.wiley.com/doi/abs/10.1049/ell2.12140

[31] R. Su, L. Dai, J. Tan, M. Hao, and R. MacKenzie, "Capacity enhancement for reconfigurable intelligent surface-aided wireless network: From regular array to irregular array," *IEEE Trans. Veh. Technol*, vol. 72, no. 5, pp. 6392–6403, 2023.

[32] J. Ye, S. Guo, and M.-S. Alouini, "Joint reflecting and precoding designs for ser minimization in reconfigurable intelligent surfaces assisted mimo systems," *IEEE Trans. Wirel. Commun.*, vol. 19, no. 8, pp. 5561–5574, 2020.

[33] H. Jiang, L. Dai, M. Hao, and R. MacKenzie, "End-to-end learning for ris-aided communication systems," *IEEE Trans. Veh. Technol*, vol. 71, no. 6, pp. 6778–6783, 2022.

[34] J. Jalali, M. Darabi, and R. C. de Lamare, "Shape adaptive reconfigurable holographic surfaces," 2025. [Online]. Available: https://arxiv.org/abs/2503.21542

[35] Q. Wu, S. Zhang, B. Zheng, C. You, and R. Zhang, "Intelligent reflecting surface-aided wireless communications: A tutorial," *IEEE Trans. .Commun.*, vol. 69, no. 5, pp. 3313–3351, 2021.

[36] O. Ozdogan, E. Bjornson, and E. G. Larsson, "Intelligent reflecting surfaces: Physics, propagation, and pathloss modeling," *IEEE Wirel. Commun. Lett.*, vol. 9, no. 5, pp. 581–585, 2020.

[37] W.-L. Guo, G.-M. Wang, X.-Y. Luo, K. Chen, H.-P. Li, and Y. Feng, "Dual-phase hybrid metasurface for independent amplitude and phase control of circularly polarized wave," *IEEE Trans. Antennas Propag.*, vol. 68, no. 11, pp. 7705–7710, 2020.

[38] H. Shi, R. Liu, Z. Zhang, X. Chen, L. Wang, J. Yi, H. Liu, and A. Zhang, "An ultrawideband 1-bit suspended reconfigurable intelligent surface for

enhancing wireless coverage," *IEEE Antennas and Wireless Propagation Letters*, vol. 23, no. 12, pp. 4613–4617, 2024.

[39] C. Pan and *et al.*, "Multicell mimo communications relying on intelligent reflecting surfaces," *IEEE Trans. Wirel. Commun.*, vol. 19, no. 8, pp. 5218–5233, 2020.

Imran A. Khoso received the M.S. degree in information and communication engineering from the University of Science and Technology Beijing, Beijing, China, in 2019, and the Ph.D. degree in communication and information systems from the Nanjing University of Aeronautics and Astronautics, Nanjing, China, in 2023. He is currently working as a postdoc researcher in Shenzhen University, Shenzhen, China. His research interests include random matrix theory, signal processing, and wireless communications. He was the recipient of various scholarships such as ICT R& D scholarship by government of Pakistan, and Chinese government scholarship.

Zhou He received the BS degree in electrical engineering from the University of Colorado Boulder, Colorado, USA, in 2018. He is currently working toward the PhD degree of mechanical engineering with the University of Maryland, College Park, USA. His research interests include wireless communication, antennas, and reliability of electronic products.

Yejun He (Senior Member, IEEE) received the Ph.D. degree in Information and Communication Engineering from the Huazhong University of Science and Technology (HUST), Wuhan, China, in 2005. From 2005 to 2006, he was a Research Associate with the Department of Electronic and Information Engineering, The Hong Kong Polytechnic University, Hong Kong. From 2006 to 2007, he was a Research Associate with the Department of Electronic Engineering, Faculty of Engineering, The Chinese University of Hong Kong, Hong Kong. In 2012, he joined the Department of Electrical and Computer Engineering, University of Waterloo, Waterloo, ON, Canada, as a Visiting Professor. From 2013 to 2015, he was an Advanced Visiting Scholar (Visiting Professor) with the School of Electrical and Computer Engineering, Georgia Institute of Technology, Atlanta, GA, USA. From 2023 to 2024, he was an Advanced Research Scholar (Visiting Professor) with the Department of Electrical and Computer Engineering, National University of Singapore, Singapore.

Since 2006, he has been a faculty of Shenzhen University, where he is currently a Full Professor with the College of Electronics and Information Engineering, Shenzhen University, Shenzhen, China, the Director of Sino-British Antennas and Propagation Joint Laboratory of Ministry of Science and Technology of the People's Republic of China (MOST), the Director of the Guangdong Engineering Research Center of Base Station Antennas and Propagation, and the Director of the Shenzhen Key Laboratory of Antennas and Propagation. He was selected as an Expert with Special Government Allowance from the State Council in China, and a Leading Talent in the "Guangdong Special Support Program" in 2024. He was promoted to the Shenzhen "Pengcheng Scholar" Distinguished Professor in 2020. He has authored or coauthored more than 330 refereed journal and conference papers and seven books. He holds more than 30 patents. His research interests include wireless communications, antennas, and radio frequency. Dr. He was also a recipient of the Shenzhen Overseas High-Caliber Personnel Level B (Peacock Plan Award B) and Shenzhen High-Level Professional Talent (Local Leading Talent). He received the Second Prize of Shenzhen Science and Technology Progress Award in 2017, the Three Prize of Guangdong Provincial Science and Technology Progress Award in 2018, the Second Prize of Guangdong Provincial Science and Technology Progress Award in 2023, and the 10th Guangdong Provincial Patent Excellence Award in 2023. He is currently the Chair of IEEE Antennas and Propagation Society-Shenzhen Chapter and obtained the 2022 IEEE APS Outstanding Chapter Award. He has served as a Technical Program Committee Member or a Session Chair for various conferences, including the IEEE Global Telecommunications Conference (GLOBECOM), the IEEE International Conference on Communications (ICC), the IEEE Wireless Communication Networking Conference (WCNC), and the IEEE Vehicular Technology Conference (VTC). He served as the TPC Chair for IEEE ComComAp 2021 and the General Chair for IEEE ComComAp 2019. He was selected as a Board Member of the IEEE Wireless and Optical Communications Conference (WOCC). He served as the TPC Co-Chair for WOCC 2023/2022/2019/2015, APCAP 2023, UCMMT 2023, ACES-China2023, NEMO 2020 and so on. He acted as the Publicity Chair of several international conferences such as the IEEE PIMRC 2012. He has served as an Executive Chair of 2024/2025 IEEE International Workshop of Radio Frequency and Antenna Technologies. He is the Principal Investigator for over 40 current or finished research projects, including the National Natural Science Foundation of China, the Science and Technology Program of Guangdong Province, and the Science and Technology Program of Shenzhen City. He has served as a Reviewer for various journals, such as the IEEE Transactions on Vehicular Technology, the IEEE Transactions on Communications, the IEEE Transactions on Industrial Electronics, the IEEE Transactions on Antennas and Propagation, the IEEE Wireless Communications, the IEEE Communications Letters, the International Journal of Communication Systems, and Wireless Personal Communications.

Dr. He is a Fellow of IET, and a Fellow of China Institute of Communications (CIC). He is serving as an Associate Editor for IEEE Transactions on Vehicular Technology, IEEE Transactions on Antennas and Propagation, IEEE Transactions on Mobile Computing, IEEE Antennas and Wireless Propagation Letters, IEEE Antennas and Propagation Magazine, International Journal of Communication Systems, China Communications, and ZTE Communications.

Mohsen Guizani (Fellow, IEEE) received the BS (with distinction), MS and PhD degrees in Electrical and Computer engineering from Syracuse University, Syracuse, NY, USA in 1985, 1987 and 1990, respectively. He is currently a Professor of Machine Learning and the Associate Provost at Mohamed Bin Zayed University of Artificial Intelligence (MBZUAI), Abu Dhabi, UAE. Previously, he worked in different institutions in the USA. His research interests include applied machine learning and artificial intelligence, Internet of Things (IoT), intelligent autonomous systems, smart city, and cybersecurity. He was elevated to the IEEE Fellow in 2009 and was listed as a Clarivate Analytics Highly Cited Researcher in Computer Science in 2019, 2020 and 2021. Dr. Guizani has won several research awards including the "2015 IEEE Communications Society Best Survey Paper Award", the Best ComSoc Journal Paper Award in 2021 as well five Best Paper Awards from ICC and Globecom Conferences. He is the author of ten books and more than 800 publications. He is also the recipient of the 2017 IEEE Communications Society Wireless Technical Committee (WTC) Recognition Award, the 2018 AdHoc Technical Committee Recognition Award, and the 2019 IEEE Communications and Information Security Technical Recognition (CISTC) Award. He served as the Editor-in-Chief of IEEE Network and is currently serving on the Editorial Boards of many IEEE Transactions and Magazines. He was the Chair of the IEEE Communications Society Wireless Technical Committee and the Chair of the TAOS Technical Committee. He served as the IEEE Computer Society Distinguished Speaker and is currently the IEEE ComSoc Distinguished Lecturer.

Mohsen Guizani (M'89–SM'99–F'09) received the BS (with distinction), MS and PhD degrees in Electrical and Computer engineering from Syracuse University, Syracuse, NY, USA in 1985, 1987 and 1990, respectively. He is currently a Professor of Machine Learning and the Associate Provost at Mohamed Bin Zayed University of Artificial Intelligence (MBZUAI), Abu Dhabi, UAE. Previously, he worked in different institutions in the USA. His research interests include applied machine learning and artificial intelligence, Internet of Things (IoT), intelligent autonomous systems, smart city, and cybersecurity. He was elevated to the IEEE Fellow in 2009 and was listed as a Clarivate Analytics Highly Cited Researcher in Computer Science in 2019, 2020 and 2021. Dr. Guizani has won several research awards including the "2015 IEEE Communications Society Best Survey Paper Award", the Best ComSoc Journal Paper Award in 2021 as well five Best Paper Awards from ICC and Globecom Conferences. He is the author of ten books and more than 800 publications. He is also the recipient of the 2017 IEEE Communications Society Wireless Technical Committee (WTC) Recognition Award, the 2018 AdHoc Technical Committee Recognition Award, and the 2019 IEEE Communications and Information Security Technical Recognition (CISTC) Award. He served as the Editor-in-Chief of IEEE Network and is currently serving on the Editorial Boards of many IEEE Transactions and Magazines. He was the Chair of the IEEE Communications Society Wireless Technical Committee and the Chair of the TAOS Technical Committee. He served as the IEEE Computer Society Distinguished Speaker and is currently the IEEE ComSoc Distinguished Lecturer.